Artificial Intelligence for Assessment of Endotracheal Tube Position on Chest Radiographs: Validation in Patients From Two Institutions

Ji Yeong An, MD[1], Eui Jin Hwang, MD, PhD[1,2], Gunhee Nam[3], Sang Hyup Lee, MD[3], Chang Min Park, MD, PhD[1,2], Jin Mo Goo, MD, PhD[1,2], Ye Ra Choi, MD[2,4]

Cardiothoracic Imaging · Original Research

Keywords

artificial intelligence, chest radiograph, deep learning, endotracheal tube, ICU

Submitted: Jun 26, 2023
Revision requested: Jul 11, 2023
Revision received: Aug 9, 2023
Accepted: Aug 31, 2023
First published online: Sep 13, 2023
Version of record: Nov 29, 2023

E. J. Hwang has received research grants from Lunit, Coreline Soft, and Monitor Corporation. C. M. Park has received a research grant from Lunit, owns stock in Promedius, and has stock options in Lunit and Coreline Soft. J. M. Goo has received research grants from Infinitt Healthcare, Dongkook Lifescience, and LG Electronics. The remaining authors declare that there are no other disclosures relevant to the subject matter of this article.

Supported by the Seoul National University Hospital Research Fund (grant no. 06-2016-3000).

BACKGROUND. Timely and accurate interpretation of chest radiographs obtained to evaluate endotracheal tube (ETT) position is important for facilitating prompt adjustment if needed.

OBJECTIVE. The purpose of our study was to evaluate the performance of a deep learning (DL)-based artificial intelligence (AI) system for detecting ETT presence and position on chest radiographs in three patient samples from two different institutions.

METHODS. This retrospective study included 539 chest radiographs obtained immediately after ETT insertion from January 1 to March 31, 2020, in 505 patients (293 men, 212 women; mean age, 63 years) from institution A (sample A); 637 chest radiographs obtained from January 1 to January 3, 2020, in 302 patients (157 men, 145 women; mean age, 66 years) in the ICU (with or without an ETT) from institution A (sample B); and 546 chest radiographs obtained from January 1 to January 20, 2020, in 83 patients (54 men, 29 women; mean age, 70 years) in the ICU (with or without an ETT) from institution B (sample C). A commercial DL-based AI system was used to identify ETT presence and measure ETT tip-to-carina distance (TCD). The reference standard for proper ETT position was TCD between greater than 3 cm and less than 7 cm, determined by human readers. Critical ETT position was separately defined as ETT tip below the carina or TCD of 1 cm or less. ROC analysis was performed.

RESULTS. AI had sensitivity and specificity for identification of ETT presence of 100.0% and 98.7% (sample B) and 99.2% and 94.5% (sample C). AI had sensitivity and specificity for identification of improper ETT position of 72.5% and 92.0% (sample A), 78.9% and 100.0% (sample B), and 83.7% and 99.1% (sample C). At a threshold *y*-axis TCD of 2 cm or less, AI had sensitivity and specificity for critical ETT position of 100.0% and 96.7% (sample A), 100.0% and 100.0% (sample B), and 100.0% and 99.2% (sample C).

CONCLUSION. AI identified improperly positioned ETTs on chest radiographs obtained after ETT insertion as well as on chest radiographs obtained of patients in the ICU at two institutions.

CLINICAL IMPACT. Automated AI identification of improper ETT position on chest radiographs may allow earlier repositioning and thereby reduce complications.

Proper endotracheal tube (ETT) positioning is critical, as an ETT positioned deep in a bronchus may lead to ipsilateral hyperventilation and contralateral atelectasis, whereas an ETT with shallow positioning may lead to extubation, air leak, or vocal cord injury [1, 2]. Clinical evaluation of ETT location—for example, using ETT measurement markings at the incisors—is inaccurate [3]. Rather, it is recommended to obtain a chest radiograph after ETT insertion to confirm proper positioning [4, 5]. Chest radiographs obtained after ETT insertion commonly show improper positioning (up to 46% of radiographs) [6–10]. The ETT tip is optimally located 5 cm above the carina when the patient is in the neutral position, although this location may vary by up to 2 cm in either direction owing to neck flexion and extension [11].

Considering the frequency and consequences of improper ETT placement, it is important to ensure timely interpretation of chest radiographs obtained after ETT insertion to allow prompt adjustment of the ETT position if needed. However, timely and accurate in-

ARRS is accredited by the Accreditation Council for Continuing Medical Education (ACCME) to provide continuing medical education activities for physicians.
The ARRS designates this journal-based CME activity for a maximum of 1.00 AMA PRA Category 1 Credit™. Physicians should claim only the credit commensurate with the extent of their participation in the activity.
Use the "Claim Credit" link to access the CME activity.

doi.org/10.2214/AJR.23.29769
AJR 2024; 222:e2329769
ISSN-L 0361-803X/24/2221–e2329769

[1]Department of Radiology, Seoul National University Hospital, 101 Daehak-ro Jongno-gu, Seoul 03080, Republic of Korea. Address correspondence to E. J. Hwang (ken921004@hotmail.com).

[2]Department of Radiology, Seoul National University College of Medicine, Seoul, Republic of Korea.

[3]Lunit, Seoul, Republic of Korea.

[4]Department of Radiology, Seoul Metropolitan Government, Seoul National University Boramae Medical Center, Seoul, Republic of Korea.

terpretation of chest radiographs obtained to evaluate ETT position may not be possible in clinical practice owing to the hectic clinical environment and heavy workload of physicians and radiologists caring for patients in ICUs [12, 13]. An artificial intelligence (AI) system that automatically determines ETT presence and location on chest radiographs obtained immediately after ETT insertion would facilitate the timely management of patients with an improperly positioned ETT.

Previous studies reported good performance of deep learning (DL)-based AI systems for the identification of improper ETT position on chest radiographs. However, these early validation studies evaluated the performance of AI systems using datasets from the same institution that provided the dataset for the AI system's development [14–18] or evaluated a dataset with an enriched prevalence of ETTs, including enriched prevalence of improperly positioned ETTs, in comparison with actual clinical practice [19–21]. Therefore, it remains uncertain whether AI systems can reproducibly identify improperly positioned ETTs in separate groups of patients with characteristics distinct from those of patients used for the AI system's development (e.g., patients with a low prevalence of improperly positioned ETTs or patients in whom chest radiographs show medical devices other than ETTs).

This study aimed to evaluate the performance of a DL-based AI system for detecting the presence and position of ETTs on chest radiographs in three patient samples from two different institutions.

Highlights

Key Finding

- *In three patient samples from two different institutions, an AI system identified ETT presence with sensitivity of 99.2–100.0% and specificity of 94.5–98.7%, improper ETT position with sensitivity of 72.5–83.7% and specificity of 92.0–100.0%, and critical ETT position with sensitivity of 100.0% in all samples and specificity of 96.7–100.0%.*

Importance

- *The AI system may allow earlier adjustment of improperly positioned ETTs, to prevent complications.*

Methods

This retrospective study was approved by the institutional review boards of the participating institutions. The requirement for informed consent from the patients was waived by the institutional review boards.

The AI system used in this study was developed by Lunit for commercial purposes. Authors who are employees of Lunit (G.N. and S.H.L.) participated in the development of the AI system. Authors not employed by Lunit (E.J.H. and J.Y.A.) had full control of the data and information submitted for publication.

Patients

The study evaluated three samples of adult patients (age ≥ 19 years): sample A, patients in the ICU, other inpatient units, or emergency department at institution A (Seoul National University Hospital, a tertiary referral institution in South Korea) who underwent chest radiography immediately after ETT insertion to assess ETT position between January 1 and March 31, 2020; sample B, patients in the ICU at institution A who underwent chest radiography between January 1 and January 3, 2020; and sample C, patients in the ICU at institution B (Seoul Metropolitan Government, Seoul National University Boramae Medical Center, a secondary referral institution in South Korea) who underwent chest radiography between January 1 and January 20, 2020. Figure 1 shows the flow of patient selection. Therefore, sample A included only chest radiographs with ETTs, whereas sample B and sample C included chest radiographs both with ETTs and without ETTs. In patients who underwent multiple chest radiography examinations meeting the inclusion criteria during the study interval, all radiographs were included in the analysis.

All chest radiographs were obtained in the anteroposterior projection using portable radiography scanners (sample A and sample B: DRX-Revolution, Carestream Health; sample C: MUX-200D-XC, Shimadzu). No digital postprocessing technique was applied to the chest radiographs before analysis.

Artificial Intelligence System

The DL algorithm for the AI system evaluated in the current study was designed to detect the presence of an ETT as well as the presence of the tracheal carina on chest radiographs and to identify the locations of the ETT tip, when present, and of the

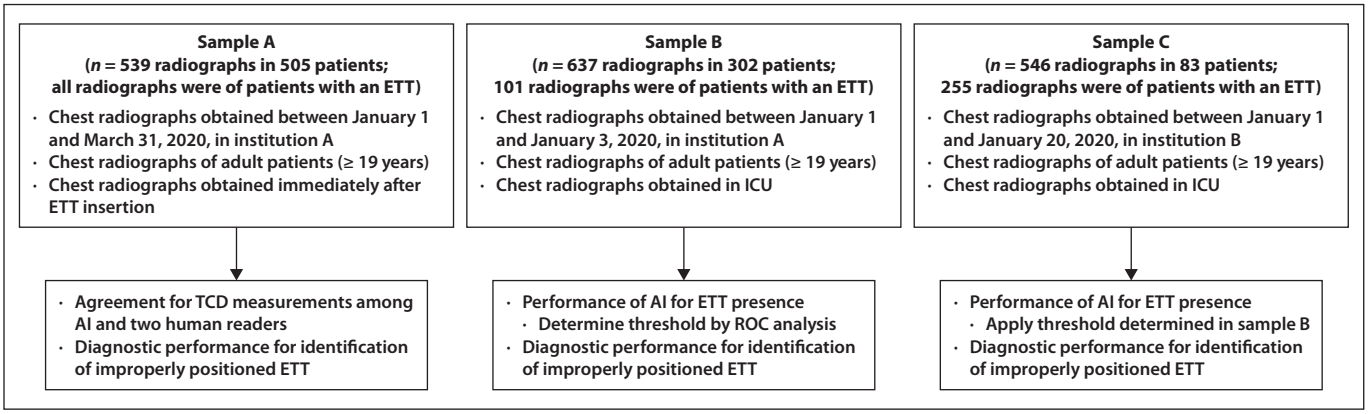

Fig. 1—Flow diagram shows patient selection. ETT = endotracheal tube, TCD = tip-to-carina distance, AI = artificial intelligence.

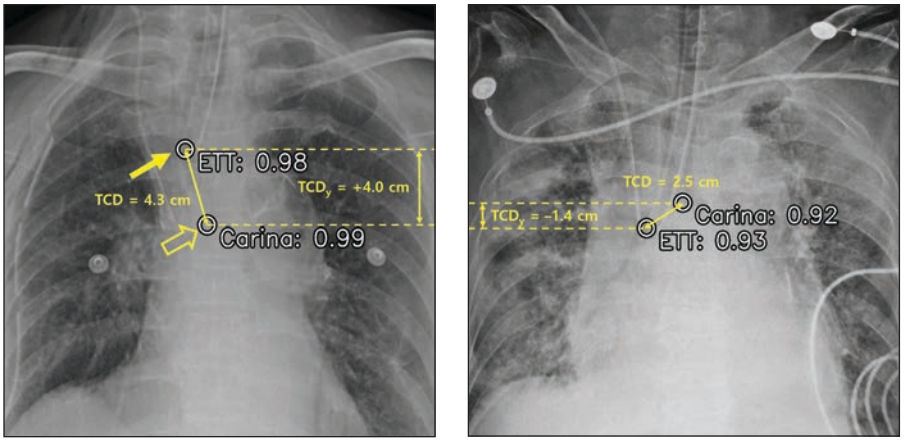

Fig. 2—Chest radiograph analyses by artificial intelligence (AI) system.
A, Chest radiograph of 80-year-old patient in sample A. AI identified endotracheal tube (ETT) (*upper circle*) with probability score of 0.98 and properly localized tip of ETT (*solid arrow*). AI also identified tracheal carina (*lower circle*) with probability score of 0.99 and properly localized carina (*open arrow*). On basis of pixel-spacing information in DICOM data header, AI automatically measured absolute distance between ETT tip and tracheal carina (tip-to-carina distance [TCD]) to be 4.3 cm. AI also measured distance between ETT tip and carina along radiograph's vertical axis (defined as *y*-axis tip-to-carina difference [TCD$_y$]) to be 4.0 cm, indicating that ETT tip is located 4.0 cm above carina. ETT is in proper position based on TCD.
B, Chest radiograph of 77-year-old patient in sample A. ETT (*lower circle*) is in critical position, with tip located below tracheal carina (*upper circle*). AI-derived TCD is 2.5 cm. AI-derived TCD$_y$ is –1.4 cm, indicating that ETT tip is located 1.4 cm below carina.

tracheal carina. The algorithm assumed that only one ETT and one tracheal carina could be present on a single chest radiograph. The algorithm's output included two probability scores (range, 0–1) for the presence of the ETT and tracheal carina, as well as the radiograph's pixel location for each of these findings [22], as shown in Figure 2. The algorithm provided a pixel location for both the ETT and tracheal carina on all radiographs regardless of the probability scores.

The algorithm was developed using approximately 100,000 chest radiographs from multiple institutions and countries that had been annotated by radiologists for the presence and location of an ETT and the tracheal carina. Chest radiographs from institution A were used to develop the algorithm. However, no patient or radiograph overlapped between the algorithm's development and the current study. Chest radiographs from institution B were not used for the algorithm's development.

On the basis of the DL algorithm's predictions and pixel-spacing information in the DICOM header data, the AI system also outputted the absolute distance between the predicted locations of the ETT tip and the tracheal carina, hereafter referred to as the tip-to-carina distance (TCD). Because the TCD was an absolute measurement, it did not indicate if the ETT was above or below the carina. The algorithm thus also determined the difference between the ETT tip and the tracheal carina along the radiograph's *y*-axis, hereafter referred to as the *y*-axis tip-to-carina difference (TCD$_y$). A positive TCD$_y$ value indicated that the ETT tip was located above the tracheal carina, whereas a negative TCD$_y$ value indicated that the ETT tip was located below the tracheal carina.

The AI system was applied to the chest radiographs in the three patient samples in the current study solely for investigational purposes. The AI results were not obtained or available at the time of the radiographs' clinical interpretation.

Image Evaluation and Reference Standard

A 2nd-year radiology resident (J.Y.A.) and a thoracic radiologist (E.J.H., 5 years of experience as an attending thoracic radiologist) reviewed chest radiographs in sample B and sample C to assess for the presence of an ETT; these assessments served as the reference standard for the presence of ETT in these two samples. For both sample B and sample C, each reader reviewed half of the radiographs in the sample, selected at random. Tracheostomy tubes present on radiographs were not considered to represent ETTs.

These same two readers independently reviewed all chest radiographs with an ETT in the three samples to measure the TCD using electronic calipers in the PACS (M6 PACS, Infinitt Healthcare) and to qualitatively record whether the ETT was located below the tracheal carina. For each radiograph with an ETT, the mean TCD between the two readers' measurements was calculated, serving as the reference standard for determining proper ETT position. In addition, discrepancies regarding the qualitative assessment for whether the ETT was located below the tracheal carina were resolved by consensus. ETTs were considered to be properly positioned when the TCD was between greater than 3 cm and less than 7 cm [11]. ETTs were considered to be improperly positioned when the TCD was 3 cm or less (deep position) or 7 cm or greater (shallow position). ETTs were considered to be in a critical position (i.e., a position possibly requiring urgent repositioning) if either the ETT tip was qualitatively assessed as located below the tracheal carina or the TCD was 1 cm or less.

After completion of the initial data analysis, the previously noted thoracic radiologist (E.J.H.) reviewed chest radiographs in sample B and sample C with a false-negative or false-positive result by AI for ETT presence, to identify possible causes for the misinterpretation.

Turnaround Time for Chest Radiograph Interpretation

The turnaround time for chest radiograph interpretation in sample B and sample C was evaluated as an indication of the time potentially required to detect an improperly positioned ETT in patients in the ICU in clinical practice and to thereby potentially decide to reposition the ETT. The turnaround time was defined as the time interval between radiograph acquisition and completion of the final radiologist report. Turnaround times were further stratified on the basis of the following subsets: all chest radiographs, chest radiographs with an ETT, chest radiographs with a properly positioned ETT, and chest radiographs with an improperly positioned ETT.

Statistical Analyses

In sample B and sample C, ROC analysis was conducted to determine the AUC of the AI's probability score for the identification

of the presence of an ETT on a chest radiograph. The threshold probability score for the presence of an ETT was determined using the Youden J statistics in sample B. Then, the sensitivity, specificity, PPV, and NPV of AI for the identification of the presence of ETT was evaluated at that threshold probability score in sample B and sample C. The agreement for TCD measurements in sample A was assessed between AI and the two human readers, as well as between the trainee and thoracic radiologist, using the mean absolute difference, intraclass correlation coefficient (ICCs), and Bland-Altman analysis. In addition, in sample A, the percentage agreement between the two human readers for whether the ETT was qualitatively below the tracheal carina was determined. The diagnostic performance of AI for identification of an improper ETT position was assessed among all chest radiographs in sample A as well as among chest radiographs with ETTs in sample B and sample C. For assessment of diagnostic performance for ETT position, the sensitivity, specificity, PPV, and NPV of the AI-derived TCD values for identification of any improper ETT position, deep ETT position, and shallow ETT position were derived, on the basis of threshold values of 3 and 7 cm for deep and shallow ETT position, respectively, using the TCD values obtained by the human readers as the reference standard.

In the three samples individually and combined, the sensitivity and PPV of deep ETT position by AI (i.e., AI-derived TCD ≤ 3 cm) for identification of subsets of deeply positioned ETTs (those with TCD ≤ 1 cm, TCD > 1 to ≤ 2 cm, and TCD > 2 cm to ≤ 3 cm, as determined by human readers) were determined; specificity and NPV were not determined given the absence of true-negatives for this analysis. ROC analysis was conducted to determine the AUC of the AI-derived TCD_y for identification of critical ETT position. Then, the sensitivity, specificity, PPV, and NPV for identification of critical ETT position were determined for TCD_y thresholds of 0 cm or less, 1 cm or less, and 2 cm or less. The median turnaround times for interpretation of chest radiographs with and without improper ETT placement were compared in sample B and sample C using the independent sample *t* test.

For our analysis, *p* values < .05 were considered statistically significant. All statistical analyses were performed using MedCalc version 20.118 (MedCalc Software).

Results

Patient Characteristics

Sample A comprised 539 chest radiographs in 505 patients (293 men, 212 women; mean age, 63 ± 15 [SD] years); sample B comprised 637 chest radiographs in 302 patients (157 men, 145 women; mean age, 66 ± 17 years); and sample C comprised 546 chest radiographs in 83 patients (54 men, 29 women; mean age, 70 ± 15 years). A total of 100.0% (*n* = 539), 15.9% (*n* = 101), and 46.7% (*n* = 255) of chest radiographs in sample A, sample B, and sample C, respectively, had an ETT. Table 1 summarizes patients' demographic and clinical characteristics.

Evaluation of Endotracheal Tube Presence in Sample B and Sample C

Table 2 summarizes the diagnostic performance of AI for the identification of ETT presence on chest radiographs in sample B and sample C, and Figure 3A shows corresponding ROC curves. In sample B, AI had an AUC for the identification of an ETT on a chest radiograph of 1.00. In sample B, the optimal threshold probability value of AI for ETT presence was 0.06. This threshold exhibited in sample B a sensitivity of 100.0% and specificity of 98.7% for identification of ETT on chest radiograph. In sample C, AI had AUC for the identification of ETT on chest radiograph of 1.00. When the threshold probability of 0.06 defined in sample B is used, AI

TABLE 1: Demographic and Clinical Characteristics

Variable	Sample A[a]	Sample B[b]	Sample C[c]
Age (y), mean ± SD	63 ± 15	67 ± 17	70 ± 15
Sex			
Male	293 (58.0)	157 (52.0)	54 (65.1)
Female	212 (42.0)	145 (48.0)	29 (34.9)
Presence of ETT	539 (100.0)	101 (15.9)	255 (46.7)
Improperly positioned ETT	153 (28.4)	19 (3.0)	43 (7.9)
Deep position	109 (20.2)	15 (2.4)	28 (5.1)
Shallow position	44 (8.2)	4 (0.6)	15 (2.7)
Critical position	22 (4.1)	2 (0.3)	5 (0.9)
Turnaround time for chest radiograph interpretation (h)			
All chest radiographs	NA	29.2 (27.0–32.1)	89.8 (87.9–91.7)
Chest radiographs with ETT	NA	31.9 (27.3–38.5)	89.8 (75.5–112.3)
Chest radiographs with improperly positioned ETT	NA	29.6 (18.4–81.6)	90.3 (65.9–137.9)
Chest radiographs with properly positioned ETT	NA	32.2 (24.2–39.4)	89.7 (67.4–112.6)

Note—Except where indicated otherwise, data are expressed as count with percentage in parentheses or as median with IQR in parentheses. Age and sex are reported at the patient level, and the remaining variables are reported at the radiograph level. ETT = endotracheal tube, NA = not applicable.

[a]Chest radiographs in sample A were obtained immediately after ETT insertion at institution A; sample A is composed of 539 radiographs in 505 patients.

[b]Chest radiographs in sample B were obtained of patients in the ICU at institution A; sample B is composed of 637 radiographs in 302 patients.

[c]Chest radiographs in sample C were obtained of patients in the ICU at institution B; sample C is composed of 546 radiographs in 83 patients.

TABLE 2: Diagnostic Performance of the AI System for the Identification of the Presence of ETT on Chest Radiograph

Measure	Sample B (*n* = 637 Radiographs)	Sample C (*n* = 546 Radiographs)
AUC	1.00 (0.99–1.00)[a]	1.00 (0.99–1.00)[a]
Sensitivity	100.0 (96.4–100.0) [101/101]	99.2 (97.2–99.9) [253/255]
Specificity	98.7 (97.3–99.5) [529/536]	94.5 (91.2–96.8) [275/291]
PPV	93.5 (87.4–96.8) [101/108]	94.1 (90.8–96.2) [253/269]
NPV	100.0 (99.3–100.0) [529/529]	99.3 (97.2–99.8) [275/277]

Note—Except where otherwise indicated, data are expressed as percentage with 95% CI in parentheses and numerator and denominator in brackets. Chest radiographs in sample B and sample C were obtained of patients in the ICU at institution A and institution B, respectively. AI = artificial intelligence, ETT = endotracheal tube.

[a]Values in parentheses indicate 95% CI.

in sample C had sensitivity of 99.2% and specificity of 94.5% for the identification of ETT on chest radiograph. Figure 4A shows a representative radiograph in a patient with a tracheostomy, with true-negative assessment by AI for ETT presence.

Of all chest radiographs combined in sample B and sample C, AI correctly classified the presence of an ETT in 97.9% (1158/1183) and incorrectly classified 2.1% (25/1183) including two false-negative assessments and 23 false-positive assessments. On the basis of a post hoc assessment, among the two chest radiographs with a false-negative identification of an ETT by AI, one showed extensive vertebral instrumentation, and the other covered only a distal short segment of the ETT. Among the 23 chest radiographs with a false-positive identification of an ETT by AI, 21 (91.3%) showed a device other than the ETT either located in the trachea (tracheostomy tube in 18) or overlapping with the trachea (nasogastric tube in three) on radiograph; no cause of the false-positive identification was identified in the remaining two cases. Figure 4B and Figure 4C show representative radiographs with false-positive and false-negative interpretations, respectively.

Agreement Among Assessments in Sample A

In sample A, the mean absolute difference for TCD measurements between the AI system and the trainee radiologist, between the AI system and the thoracic radiologist, and between the trainee and the thoracic radiologist, were 5.2 ± 5.7 (SD) mm, 6.2 ± 5.2 mm, and 5.1 ± 4.6 mm, respectively. ICC of TCD measurements for the AI system and trainee radiologist, the AI system and thoracic radiologist, and the trainee and thoracic radiologist were 0.92, 0.91, and 0.93, respectively. Figure 5 shows the Bland-Altman plots for agreement of TCD measurements between the AI system and each of the two human readers as well as between the TCD measurements and the two human readers.

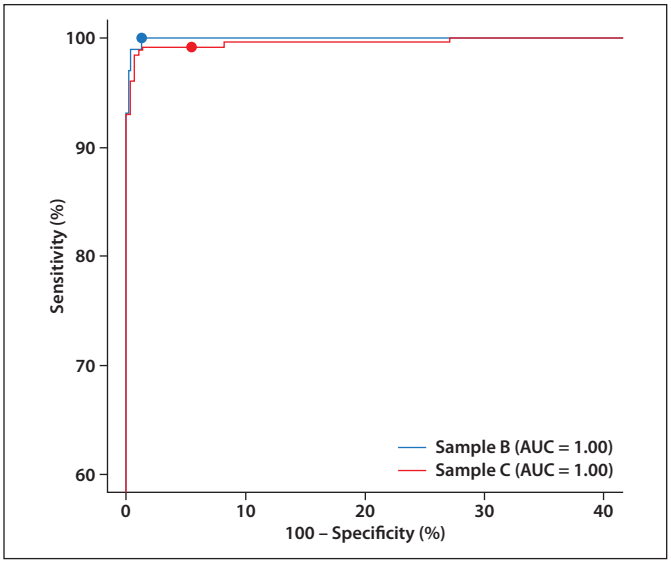

A

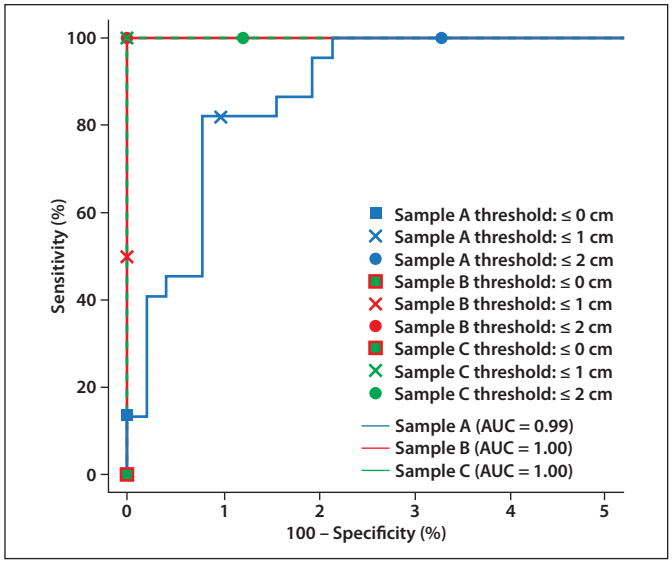

B

Fig. 3—ROC curves show diagnostic performance of artificial intelligence (AI) system.

A, ROC curves show diagnostic performance of AI system for identification of presence of endotracheal tube (ETT) on chest radiograph in sample B and sample C. AUC was 1.00 in both samples.

B, ROC curves show diagnostic performance of AI system for identification of critical ETT position on chest radiograph in sample A, sample B, and sample C. AUC in three samples ranged from 0.99 to 1.00. Diagnostic performance in each sample at threshold *y*-axis tip-to-carina difference (TCD_y) values of 0 cm or less, 1 cm or less, and 2 cm or less are marked. At threshold TCD_y value of 2 cm or less, AI detected critical ETT position with sensitivity of 100.0% and specificity of 96.7–100.0% in three samples.

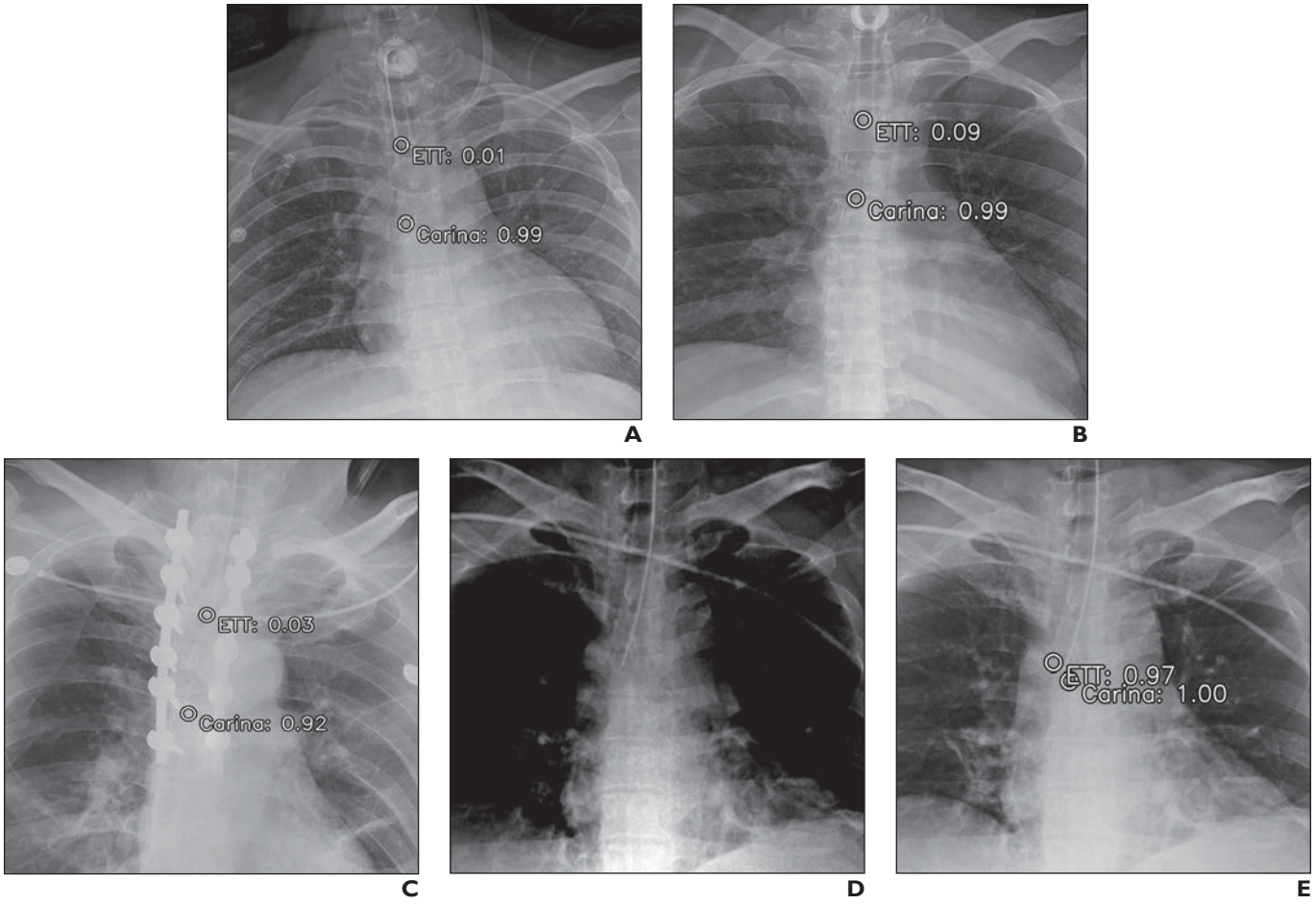

Fig. 4—Chest radiographs of representative patients.
A, Chest radiograph of 21-year-old patient in sample B. Tracheostomy tube is present in trachea. Artificial intelligence (AI) yielded probability score for presence of endotracheal tube (ETT) (*upper circle*) of 0.01, below threshold of 0.06 for ETT detection, consistent with true-negative result. AI also identified tracheal carina (*lower circle*) with probability score of 0.99.
B, Chest radiograph of 21-year-old patient in sample B. Tracheostomy tube is present in trachea. AI yielded probability score for presence of ETT (*upper circle*) of 0.09, above threshold of 0.06 for ETT detection, consistent with false-positive result, attributed to presence of tracheostomy. AI also identified tracheal carina (*lower circle*) with probability score of 0.99.
C, Chest radiograph of 64-year-old patient in sample C. Surgical fixation hardware is present in thoracic spine. ETT (*upper circle*) is also present. AI yielded probability score for presence of ETT of 0.03, below threshold of 0.06 for ETT detection, consistent with false-negative result. AI also identified tracheal carina (*lower circle*) with probability score of 0.92.
D and **E,** Chest radiographs of 56-year-old patient in sample A without (**D**) and with (**E**) AI results. ETT tip was assessed by human readers as below tracheal carina, consistent with critical position. AI yielded probability score for presence of ETT (*upper circle*, **E**) of 0.97 and also identified tracheal carina (*lower circle*, **E**) with probability score of 1.00. AI-derived *y*-axis tip-to-carina difference (TCD_y) is 1.3 cm, consistent with critical position at threshold TCD_y of 2 cm or less.

The two human readers agreed regarding whether the ETT was qualitatively below the tracheal carina in 537 of 539 (99.6%) radiographs in sample A; of the two radiographs with a discrepancy for this assessment, the consensus assessment was that the ETT was above the tracheal carina on one radiograph and below the tracheal carina on one radiograph.

Evaluation of Endotracheal Tube Position in All Three Samples

Table 1 summarizes information regarding the frequency of improper ETT position in the three samples. According to the reference standard (mean of the two human readers' TCD measurements), the ETT was improperly positioned (TCD ≤ 3 cm or TCD ≥ 7 cm) in 28.4% (153/539), 18.8% (19/101), and 16.9% (43/255) of chest radiographs with an ETT in sample A, sample B, and sample C, respectively. Deep ETT position (TCD ≤ 3 cm) was observed in 109, 15, and 28 chest radiographs in sample A, sample B, and sample C; shallow ETT position (TCD ≥ 7 cm) was observed in 44, 4, and 15 chest radiographs, in sample A, sample B, and sample C.

Table 3 summarizes the diagnostic performance of AI for the identification of improperly positioned ETT in the three samples. The AI system had a sensitivity and specificity for identification of improper ETT position of 72.5% and 92.0% in sample A, 78.9% and 100.0% in sample B, and 83.7% and 99.1% in sample C, respectively. The AI system had a sensitivity and specificity for identification of shallow ETT position of 88.6% and 94.3% in sample A, 100.0% and 100.0% in sample B, and 93.3% and 99.6% in sample C. The AI system had a sensitivity and specificity for identification of deep ETT position of 66.1% and 99.3% in sample A, 73.3% and 100.0% in sample B, and 78.6% and 99.6% in sample C.

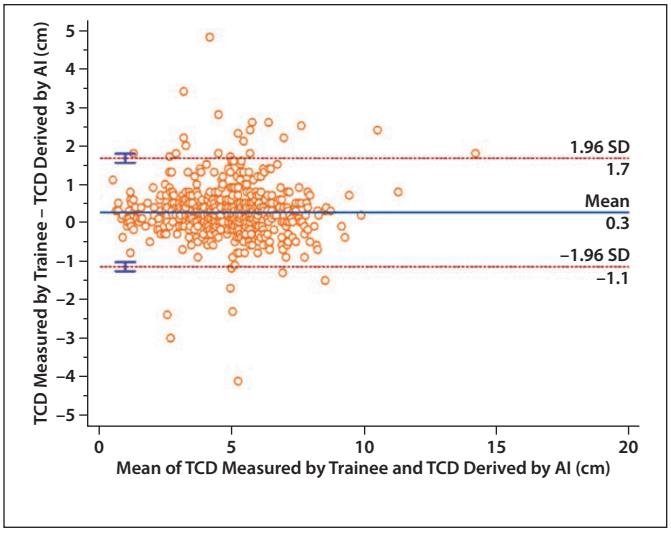

A

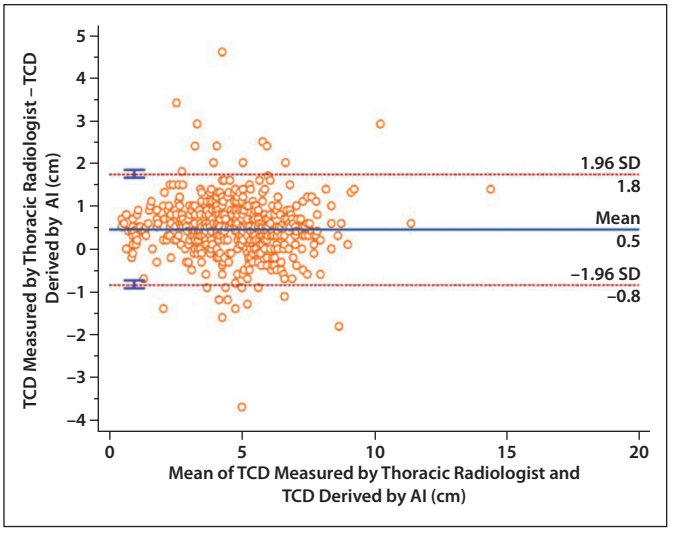

B

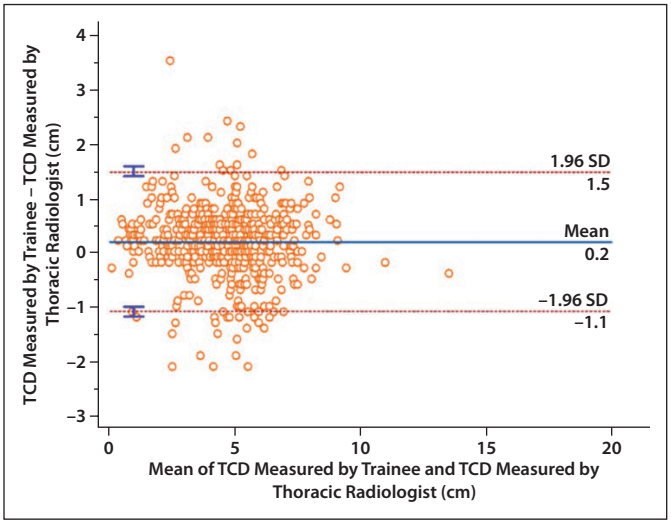

C

Fig. 5—Bland-Altman plots for agreement of tip-to-carina distance (TCD) measurements in sample A.
A–C, Bland-Altman plots for agreement of TCD measurements between artificial intelligence (AI) system and trainee (**A**; 95% limits of agreement, 1.7 and –1.1 cm), AI system and thoracic radiologist (**B**; 95% limits of agreement, 1.8 and –0.8 cm), and trainee and thoracic radiologist (**C**; 95% limits of agreement, 1.5 and –1.1 cm) show similar degree of agreement for all assessments. Whiskers show 95% limits of agreement.

Table 4 summarizes the diagnostic performance of AI for the identification of deep ETTs based on ranges of TCD measurements. In the three samples combined, deep ETT position based on AI (i.e., AI-derived TCD ≤ 3 cm) had sensitivity and PPV of 69.1% and 100.0% for all deep ETTs, 100.0% and 100.0% for deep ETTs with TCD of 1 cm or less, 90.0% and 100.0% for deep ETTs with TCD greater than 1 cm to 2 cm or less, and 50.0% and 100.0% for deep ETTs with TCD greater than 2 cm to 3 cm or less.

The ETT had a critical position in 22, two, and five chest radiographs in sample A, sample B, and sample C, respectively. Figure 3B shows ROC curves for identification of critical ETT position by AI-derived TCD_y values and also depicts threshold TCD_y values on the curves. The AI-derived TCD_y value had AUC for identification of critical ETT position of 0.99, 1.00, and 1.00 in sample A, sample B, and sample C. Table 3 summarizes the diagnostic performance of AI for the identification of ETTs with critical position based on various TCD_y thresholds. At a threshold TCD_y of 0 cm or less, AI had sensitivity and specificity for critical ETT position of 13.6% and 100.0% in sample A, 0.0% and 100.0% in sample B, and 0.0% and 100.0% in sample C. At a threshold TCD_y of 2 cm or less, AI had sensitivity and specificity for critical ETT position of 100.0% and 96.7% in sample A, 100.0% and 100.0% in sample B, and 100.0% and 99.2%, in sample C. Figures 4D and 4E show an ETT with critical position that was correctly identified by AI.

Turnaround Time for Chest Radiograph Interpretation in Sample B and Sample C

Table 1 summarizes the turnaround times for chest radiograph interpretation in sample B and sample C. The median turnaround time for the clinical chest radiograph interpretations was 29.2 hours in sample B and 89.8 hours in sample C. The median turnaround time was not significantly different between chest radiographs with improper and proper ETT position in sample B (29.6 vs 32.2 hours, respectively; $p = .92$) or sample C (90.3 vs 89.7 hours; $p = .37$).

Discussion

AI systems have been explored for the automated evaluation of ETTs on chest radiographs to aid early detection and time-

TABLE 3: Diagnostic Performance of the AI System for the Identification of Improperly Positioned ETT on Chest Radiograph

Outcome and Measure	Sample A (*n* = 539 ETTs on 539 Radiographs)	Sample B (*n* = 101 ETTs on 637 Radiographs)	Sample C (*n* = 255 ETTs on 546 Radiographs)
Identification of any improper ETT position			
Sensitivity	72.5 (64.8–79.4) [111/153]	78.9 (54.4–93.9) [15/19]	83.7 (69.3–93.2) [36/43]
Specificity	92.0 (88.8–94.5) [355/386]	100.0 (95.6–100.0) [82/82]	99.1 (96.6–99.9) [210/212]
PPV	78.2 (71.6–83.6) [111/142]	100.0 (78.2–100.0) [15/15]	94.7 (93.8–98.3) [36/38]
NPV	89.4 (86.7–91.6) [355/397]	95.3 (89.6–98.0) [82/86]	96.8 (93.8–98.3) [210/217]
Identification of deep ETT position			
Sensitivity	66.1 (56.4–74.9) [72/109]	73.3 (44.9–92.2) [11/15]	78.6 (59.0–91.7) [22/28]
Specificity	99.3 (98.0–99.9) [427/430]	100.0 (95.8–100.0) [86/86]	99.6 (97.6–100.0) [226/227]
PPV	96.0 (89.9–93.7) [72/75]	100.0 (71.5–100.0) [11/11]	95.7 (75.5–99.4) [22/23]
NPV	92.0 (89.9–93.7) [427/464]	95.6 (90.3–98.0) [86/90]	97.4 (94.4–98.9) [226/232]
Identification of shallow ETT position			
Sensitivity	88.6 (75.4–96.2) [39/44]	100.0 (39.8–100.0) [4/4]	93.3 (68.1–99.8) [14/15]
Specificity	94.3 (91.9–96.2) [467/495]	100.0 (96.3–100.0) [97/97]	99.6 (97.7–100.0) [239/240]
PPV	58.2 (48.9–67.0) [39/67]	100.0 (39.8–100.0) [4/4]	93.3 (66.3–99.0) [14/15]
NPV	98.9 (97.6–99.5) [467/472]	100.0 (96.3–100.0) [97/97]	99.6 (97.3–99.9) [239/240]
Identification of critical ETT position based on threshold $TCD_y \leq 0$ cm			
Sensitivity	13.6 (2.9–34.9) [3/22]	0.0 (0.0–84.2) [0/2]	0.0 (0.0–52.2) [0/5]
Specificity	100.0 (99.3–100.0) [517/517]	100.0 (96.3–100.0) [99/99]	100.0 (98.5–100.0) [250/250]
PPV	100.0 (29.2–100.0) [3/3]	NA[a]	NA[a]
NPV	96.5 (95.8–97.0) [517/536]	98.0 (98.0–98.0) [99/101]	98.0 (95.5–99.4) [250/255]
Identification of critical ETT position based on threshold $TCD_y \leq 1$ cm			
Sensitivity	81.8 (89.7–94.8) [18/22]	50.0 (1.3–98.7) [1/2]	80.0 (28.4–99.5) [4/5]
Specificity	99.0 (97.8–99.7) [512/517]	100.0 (96.3–100.0) [99/99]	100.0 (98.5–100.0) [250/250]
PPV	78.3 (59.5–89.8) [18/23]	100.0 (2.5–100.0) [1/1]	100.0 (39.8–100.0) [4/4]
NPV	99.2 (98.1–99.7) [512/516]	99.0 (96.1–99.7) [99/100]	99.6 (97.7–99.9) [250/251]
Identification of critical ETT position based on threshold $TCD_y \leq 2$ cm			
Sensitivity	100.0 (84.6–100.0) [22/22]	100.0 (15.8–100.0) [2/2]	100.0 (47.8–100.0) [5/5]
Specificity	96.7 (94.8–98.1) [500/517]	100.0 (96.3–100.0) [99/99]	99.2 (97.1–99.9) [248/250]
PPV	56.4 (44.8–67.4) [22/39]	100.0 (15.8–100.0) [2/2]	71.4 (38.6–90.9) [5/7]
NPV	100.0 (99.3–100.0) [500/500]	100.0 (96.3–100.0) [99/99]	100.0 (98.5–100.0) [248/248]

Note—Data are expressed as percentage with 95% CI in parentheses and numerator and denominator in brackets. Chest radiographs in sample A were obtained immediately after ETT insertion at institution A; radiographs in sample B and sample C were obtained of patients in the ICU at institution A and institution B, respectively. AI = artificial intelligence, ETT = endotracheal tube, TCD_y = *y*-axis tip-to-carina difference, NA = not applicable.
[a]No radiograph was assessed by AI as positive for critical ETT position based on provided threshold.

ly management of improperly positioned ETTs. In contrast with previous studies that mainly investigated AI performance in single samples for detecting the presence of ETT without assessing TCD or proper positioning [18, 20], this study focused on assessment of TCD and TCD_y, as well as subcategories of improperly positioned ETTs, in three patient samples representing various clinical situations. The AI system's performance was evaluated for identifying ETTs and measuring TCD on chest radiographs obtained immediately after ETT insertion and on chest radiographs obtained in patients in the ICUs of two different institutions. The AI system identified the presence of ETT with sensitivity of 99.2–100.0% and specificity of 94.5–98.7% and identified improper ETT position with sensitivity of 72.5–83.7% and specificity of 92.0–100.0%.

Measuring the TCD is essential for evaluating ETT position [1, 23]. In this study, the AI system measured TCD with a high level of

TABLE 4: Diagnostic Performance of Deep ETT Position by AI[a] for Identification of Subsets of Deeply Positioned ETTs Based on Ranges of TCD, as Determined by Human Readers

TCD Range of Deep ETTs	Sample A		Sample B		Sample C		All Samples	
	Sensitivity	PPV	Sensitivity	PPV	Sensitivity	PPV	Sensitivity	PPV
≤ 1 cm	100.0 (82.4–100.0) [19/19]	100.0 (82.4–100.0) [19/19]	100.0 (15.8–100.0) [2/2]	100.0 (15.8–100.0) [2/2]	100.0 (47.8–100.0) [5/5]	100.0 (47.8–100.0) [5/5]	100.0 (86.8–100.0) [26/26]	100.0 (86.8–100.0 [26/26]
> 1 cm to ≤ 2 cm	86.2 (68.3–96.1) [25/29]	100.0 (86.3–100.0) [25/25]	100.0 (15.8–100.0) [2/2]	100.0 (15.8–100.0) [2/2]	100.0 (66.4–100.0) [9/9]	100.0 (66.4–100.0) [9/9]	90.0 (76.3–97.2) [36/40]	100.0 (90.3–100.0) [36/36]
> 2 cm to ≤ 3 cm	45.9 (33.1–59.2) [28/61]	100.0 (87.7–100.0) [28/28]	63.6 (30.8–89.1) [7/11]	100.0 (59.0–100.0) [7/7]	57.1 (28.9–82.3) [8/14]	100.0 (63.1–100.0) [8/8]	50.0 (39.0–61.0) [43/86]	100.0 (91.8–100.0) [43/43]
≤ 3 cm (all deep ETTs)	66.1 (56.4–74.9) [72/109]	100.0 (95.0–100.0) [72/72]	73.3 (44.9–92.2) [11/15]	100.0 (71.5–100.0) [11/11]	78.6 (59.0–91.7) [22/28]	100.0 (84.6–100.0) [22/22]	69.1 (61.1–76.3) [105/152]	100.0 (96.5–100.0) [105/105]

Note—Data are expressed as percentage with 95% CI in parentheses and numerator and denominator in brackets. ETT = endotracheal tube, AI = artificial intelligence, TCD = tip-to-carina distance.
[a]Deep ETT position is defined as AI-derived TCD ≤ 3 cm.

agreement with two human readers (mean absolute difference, 5.2–6.2 mm; ICC, 0.91–0.92), similar to the agreement between the two human readers (mean absolute difference, 5.1 mm; ICC, 0.93). The agreement in this study was comparable with those reported in previous studies (mean absolute error, 7 mm; ICC, 0.84–0.89 [16]; mean absolute error, 4.8–6.0 mm; ICC, 0.87–0.92 [24]). In this study, we defined the reference standard for proper ETT position as TCD between greater than 3 cm and less than 7 cm, on the basis of the mean value of the two human readers' measurements [1, 11]. Although the optimal position of the ETT tip and the need for repositioning may vary on the basis of patient height and neck position, we believe that the range of TCD of 3–7 cm may provide a sufficient safety margin. If AI can alert radiologists and ICU physicians when the TCD is outside this range, then the radiologist or ICU physician can promptly evaluate the chest radiograph in the context of the patient's neck position to confirm the necessity for ETT repositioning. On the basis of the threshold criteria (TCD of 3–7 cm), the AI exhibited sensitivity of 72.5–83.7% and specificity of 92.0–100.0% for identification of improper ETT position, comparable with performance values reported in prior studies (sensitivity of 66.5–93.9% and specificity of 92.4–97.7% [16]; sensitivity of 95% [20]). A potential major source of misclassification by AI regarding ETT position is inappropriate localization of the tracheal carina and ETT tip. Given that the ETT tip is beveled, localizing the exact distalmost point of the ETT may be a difficult task for both AI and human readers. Although the AI system exhibited limited sensitivity for all deep ETTs (69.1%), it had excellent sensitivity for deep ETTs with TCD of 1 cm or less (100.0%) or for deep ETTs with TCD of greater than 1 cm to 2 cm or less (90.0%), indicating higher sensitivity of AI for more clinically relevant improperly positioned ETTs.

Urgent repositioning of the ETT may be required if the ETT tip is located in the mainstem bronchi or just above the tracheal carina. We defined ETTs as being in critical position if the ETT tip was located below the tracheal carina or if the TCD was 1 cm or less. Given that AI-derived absolute TCD measurements do not indicate whether ETTs are located beyond the carina, we used AI-derived TCD_y values to identify critical ETT positions, whereby a negative TCD_y value indicates that the ETT tip is below the level of the trachea. In ROC analysis, AI-derived TCD_y values exhibited AUCs of 0.99–1.00 for identification of critical ETT positions. At the threshold TCD_y value of 2 cm or less, AI exhibited sensitivity of 100.0% and specificity of 96.7–100.0%. We believe that if AI can provide an urgent alert to ICU physicians that a patient has an ETT with TCD_y value of 2 cm or less, then AI may ultimately help achieve timely intervention to prevent complications from the improper position, with an acceptable number of false-positive alerts.

Identification of the presence of an ETT on a chest radiograph is an essential step in the automated evaluation of ETT position, as chest radiographs both with and without ETTs are encountered in clinical practice. The AI system had an AUC for discrimination of chest radiographs with and without ETTs of 1.00 among chest radiographs obtained from the ICUs of two different institutions. However, AI misclassified the presence of ETT in 2.1% of chest radiographs. Twenty-three of a total of 25 (92.0%) misclassifications were false-positive identifications of ETTs and were associated with devices other than ETT located in the trachea (tracheostomy tubes) or overlapping with the trachea on chest radiograph (nasogastric tube). Medical devices other than ETTs are commonly observed on chest radiographs in patients in the ICU and can influence AI's diagnostic performance.

A key strength of this study is the demonstration of consistent performance by the AI system in different patient samples and institutions. Given that improper ETT location is most commonly encountered immediately after ETT insertion, it is recommended to obtain a chest radiograph after ETT insertion to confirm proper position [4, 5]. Sample A comprised consecutive chest radiographs obtained immediately after ETT insertion; thus, the frequency of improper ETT position in this sample is expected to reflect the frequency of improper ETT position among radiographs obtained for this indication in a real-world setting. Therefore, the performance of AI in sample A provides important evidence supporting the clinical utility of this AI system for assessing ETT position after ETT insertion in clinical practice. In comparison, sample B and sample C comprised chest radiographs obtained of patients in the ICUs of two different institutions and reflected the prevalence of ETT presence and of improper ETT position, as well as the spectrum of imaging characteristics of patients in the ICU, in clinical practice. Some of

these patients may have ETTs, whereas others may not. Patients also commonly have various medical devices other than ETTs, and appropriate patient positioning during chest radiograph acquisition can be difficult. In this regard, the performance of AI in sample B and sample C provides important insight into the AI system's efficacy in patients in the ICU.

Timely interpretation of chest radiographs is a key component for the management of patients with an improperly positioned ETT. The median turnaround times for the interpretation of chest radiographs of patients in the ICU in the current study (29.2 and 89.8 hours for all chest radiographs and 29.6 and 90.3 hours for chest radiographs with an improperly positioned ETT in sample B and sample C, respectively) were suboptimal for achieving timely patient management. These long delays may relate to radiologist workforce shortages and large examination volumes at the two study institutions, leading to heavy workloads for individual radiologists. Radiologists may focus on timely interpretation of CT and MRI examinations, which generally require formal radiologist interpretation to guide clinical decision-making, whereas interpretation of chest radiographs may be delayed because referring clinicians may assess and act on the radiographs without formal radiologist interpretation. In this situation, AI may help achieve timely chest radiograph interpretation and patient management via the automated evaluation of chest radiographs immediately after image acquisition, with subsequent notification of referring clinicians and radiologists when improper ETT position is suspected.

This study had limitations. First, it remains unclear whether the AI system's performance can be reproduced in clinical practice given that the AI system was applied to chest radiographs retrospectively. Second, it is unclear whether the use of AI will result in earlier repositioning of ETTs in clinical practice, as automated identification of improper ETT position on chest radiograph is only an initial step of a process; notification of the radiologist or referring clinician and subsequent timely intervention to correct the improper position remain necessary. Third, the performance of AI in institution A may be biased because chest radiographs from this institution were used for the AI system's development. Further validation of the AI system in different patient groups from different institutions or nations is required to confirm the generalizability of the results. Fourth, because we evaluated a specific AI system, the results cannot be generalized to other AI systems. Fifth, the TCD measurement by radiologists, used as this study's reference standard, may vary across radiologists. Sixth, the analysis did not account for possible clustering effects among multiple radiographs in individual patients. Finally, patients' neck position and symmetry of the radiographs were not evaluated.

In conclusion, this study showed the ability of an AI system to identify the position of the ETT tip on chest radiographs obtained after ETT insertion as well as on chest radiographs obtained of patients in the ICU at two institutions. Further investigation is required to evaluate whether the AI system can be implemented in clinical practice to automatically identify patients with an improperly positioned ETT and help achieve timely patient management.

Provenance and review: Not solicited; externally peer reviewed.

Peer reviewers: Diana Litmanovich, Beth Israel Lahey Health, Harvard Medical School; additional individual(s) who chose not to disclose their identity.

References

1. Goodman LR, Conrardy PA, Laing F, Singer MM. Radiographic evaluation of endotracheal tube position. *AJR* 1976; 127:433–434
2. Hyzy RC, Manaker S, Finlay G. Complications of the endotracheal tube following initial placement: prevention and management in adult intensive care unit patients. *Crit Care Med* 2017; 24:25
3. Wang ML, Schuster KM, Bhattacharya B, Maung AA, Kaplan LJ, Davis KA. Repositioning endotracheal tubes in the intensive care unit: depth changes poorly correlate with postrepositioning radiographic location. *J Trauma Acute Care Surg* 2013; 75:146–149
4. Laroia AT, Donnelly EF, Henry TS, et al.; Expert Panel on Thoracic Imaging. ACR Appropriateness Criteria: intensive care unit patients. *J Am Coll Radiol* 2021; 18(suppl 5):S62–S72
5. Tolsma M, Rijpstra TA, Schultz MJ, Mulder PG, van der Meer NJ. Significant changes in the practice of chest radiography in Dutch intensive care units: a web-based survey. *Ann Intensive Care* 2014; 4:10
6. Strain DS, Kinasewitz GT, Vereen LE, George RB. Value of routine daily chest x-rays in the medical intensive care unit. *Crit Care Med* 1985; 13:534–536
7. Gray P, Sullivan G, Ostryzniuk P, McEwen TA, Rigby M, Roberts DE. Value of postprocedural chest radiographs in the adult intensive care unit. *Crit Care Med* 1992; 20:1513–1518
8. Marik PE, Janower ML. The impact of routine chest radiography on ICU management decisions: an observational study. *Am J Crit Care* 1997; 6:95–98
9. Brunel W, Coleman DL, Schwartz DE, Peper E, Cohen NH. Assessment of routine chest roentgenograms and the physical examination to confirm endotracheal tube position. *Chest* 1989; 96:1043–1045
10. O'Brien W, Karski JM, Cheng D, Carroll-Munro J, Peniston C, Sandler A. Routine chest roentgenography on admission to intensive care unit after heart operations: is it of any value? *J Thorac Cardiovasc Surg* 1997; 113:130–133
11. Godoy MC, Leitman BS, de Groot PM, Vlahos I, Naidich DP. Chest radiography in the ICU. Part 1. Evaluation of airway, enteric, and pleural tubes. *AJR* 2012; 198:563–571
12. Mortani Barbosa EJ Jr, Lynch MC, Langlotz CP, Gefter WB. Optimization of radiology reports for intensive care unit portable chest radiographs. *J Thorac Imaging* 2016; 31:43–48
13. Rachh P, Levey AO, Lemmon A, et al. Reducing STAT portable chest radiograph turnaround times: a pilot study. *Curr Probl Diagn Radiol* 2018; 47:156–160
14. Huang MH, Chen C-Y, Horng MH, et al. Validation of a deep learning–based automatic detection algorithm for measurement of endotracheal tube-to-carina distance on chest radiographs. *Anesthesiology* 2022; 137:704–715
15. Chen S, Zhang M, Yao L, Xu W. Endotracheal tubes positioning detection in adult portable chest radiography for intensive care unit. *Int J CARS* 2016; 11:2049–2057
16. Lakhani P, Flanders A, Gorniak R. Endotracheal tube position assessment on chest radiographs using deep learning. *Radiol Artif Intell* 2020; 3:e200026
17. Brown MS, Wong K-P, Shrestha L, et al. Automated endotracheal tube placement check using semantically embedded deep neural networks. *Acad Radiol* 2023; 30:412–420
18. Kara S, Akers JY, Chang PD. Identification and localization of endotracheal tube on chest radiographs using a cascaded convolutional neural network approach. *J Digit Imaging* 2021; 34:898–904
19. Oliver M, Renou A, Allou N, Moscatelli L, Ferdynus C, Allyn J. Image augmentation and automated measurement of endotracheal-tube-to-carina distance on chest radiographs in intensive care unit using a deep learning model with external validation. *Crit Care* 2023; 27:40
20. Lakhani P. Deep convolutional neural networks for endotracheal tube po-

sition and X-ray image classification: challenges and opportunities. *J Digit Imaging* 2017; 30:460–468

21. Harris RJ, Baginski SG, Bronstein Y, et al. Measurement of endotracheal tube positioning on chest x-ray using object detection. *J Digit Imaging* 2021; 34:846–852
22. Nam G, Kim T, Lee S, Kooi T. OOOE: Only-one-object-exists assumption to find very small objects in chest radiographs. In: *Applications of Medical Artificial Intelligence: First International Workshop, AMAI 2022, Held in Conjunction with MICCAI 2022, Singapore, September 18, 2022, Proceedings*. Springer, 2022:139–149
23. Lal A, Pena ED, Sarcilla DJ, Perez PP, Wong JC, Khan FA. Ideal length of oral endotracheal tube for critically ill intubated patients in an Asian population: comparison to current Western standards. *Cureus* 2018; 10:e3590
24. Schultheis WG, Lakhani P. Using deep learning segmentation for endotracheal tube position assessment. *J Thorac Imaging* 2022; 37:125–131

Editorial Comment: Artificial Intelligence for Detection of Endotracheal Tube Malposition—Augmented Rather Than Autonomous Radiology Interpretation

Many artificial intelligence (AI) applications in radiology are designed to augment rather than replace human image interpretation, more like the safety features of a conventional automobile than a completely automated, self-driving vehicle. While debates continue about the role AI will play in the future of medical imaging, this study highlights the value of a targeted AI system for flagging urgent findings such as abnormal endotracheal tube (ETT) position.

In this multicenter retrospective study, an AI system showed high accuracy for detection of critically low ETT positions. For positions lower than 2 cm above the carina (including mainstem intubation), the AI system had a sensitivity of 100.0% across three centers and a specificity of 96.7–100.0%. As AI performance can be heavily influenced by the composition of the training and testing groups, such robust results across institutions are reassuring. However, even a dedicated AI algorithm designed to perform a seemingly straightforward task showed suboptimal overall sensitivity of 72.5–83.7% for the detection of any ETT malposition, defined as either 3 cm or less or 7 cm or more above the carina. Such an algorithm should be considered a safety feature serving as an early warning system and a second check on human interpretation of ETT position rather than an automated arbiter of correct position.

Prompt diagnosis is paramount when assessing the value of AI for the detection of urgent findings such as ETT malposition. Although the final report turnaround times in this study seem much longer than the norm (median of up to ≈ 90 hours), the study highlights the strong temporal advantages of AI-assisted early warning systems. As with always-on collision avoidance and other safety features of automobiles and airplanes, both accuracy and immediacy are important for avoiding adverse consequences in medicine and can be elegantly delivered by AI systems working in concert with human interpretation.

Brent P. Little, MD
Mayo Clinic Florida
Jacksonville, FL
little.brent@mayo.edu, @bplittle

Version of record: Nov 29, 2023

The author declares that there are no disclosures relevant to the subject matter of this article.

doi.org/10.2214/AJR.23.30297 ▪ *AJR* 2024; 222:e2330297

ISSN-L 0361-803X/24/2221–e2330297 ▪ © American Roentgen Ray Society

Provenance and review: Solicited; not externally peer reviewed.